Electronic Supplementary Material (ESI) for Lab on a Chip.

Supporting Information

Magnetofluid-Integrated Biosensors Based on DNase-dead Cas12a for Visual Point-of-Care Testing of HIV-1 by Up & Down Chip

Di Huang,[a,b] Yekai Zhao[a,b], Mengjun Fang,[a,b] Peijie Shen,[a,b] Hu Xu,[a,b] Yichen He,[a,b] Shengfu Chen,[a,c] Zhenjun Si[d], Zhinan Xu[a,b,*]

[a] *Key Laboratory of Biomass Chemical Engineering of Ministry of Education, College of Chemical and Biological Engineering, Zhejiang University, Hangzhou 310027, China.*

[b] *Institute of Biological Engineering, College of Chemical and Biological Engineering, Zhejiang University, Hangzhou 310027, China.*

[c] *Institute of Pharmaceutical Engineering, College of Chemical and Biological Engineering, Zhejiang University, Hangzhou 310027, China.*

[d] *Hangzhou FasTech Biotechnology Company Limited, Hangzhou 310005, China.*

*Corresponding author:
Prof. Zhinan Xu (znxu@zju.edu.cn)

Table of Contents

DNase-dead Cas12a expression and purification

The DNase-dead Cas12a (dCas12a) variant utilized in this study was expressed heterologously in *E. coli* BL21 (DE3) from a codon-optimized synthetic gene and purified through a combination of Ni^{2+}-affinity chromatography and ultrafiltration desalination. Specifically, the gene sequence was synthesized and inserted into the pET28a plasmid by ligation-independent cloning to generate a protein expression construct encoding the dCas12a polypeptide sequence (Table S2) fused with an N-terminal hexahistidine tag. When cultures were grown in Terrific Broth medium at 37 ℃ to an OD600 nm of 2.0, cells were induced by 0.1 mM isopropyl-1-thio-β-D-galactopyranoside (IPTG) and incubated at 18 ℃ for 8 h. The resulting cells were harvested by centrifugation, and the pellet was resuspended in Buffer A (20 mM Tris-HCl, 300 mM NaCl, 10 mM imidazole, pH 7.5). Then the cells were lysed via sonication, and the insoluble residues were removed through centrifugation. The clarified supernatant was applied to a column with Ni Sepharose (GE Healthcare) which was pre-equilibrated by Buffer A. After washing by 10 column volumes of Buffer B (20 mM Tris-HCl, 300 mM NaCl, 50 mM imidazole, pH 7.5) to remove nonspecifically bound proteins in the resin, the recombinant dCas12a eluted using Buffer C (20 mM Tris-HCl, 300 mM NaCl, 250 mM imidazole, pH 7.5). The obtained product was cleaned and desalted using a 100 kDa cutoff ultrafiltration membrane, and then the buffer was exchanged to Buffer D (40 mM Tris-HCl, 600 mM NaCl, 2 mM DTT, pH 7.5). Finally, the dCas12a solution was collected and concentrated to a final concentration of 10 μM and stored at -20 °C with the supplement of 50% glycerol.

Enhanced green fluorescent protein expression and purification

The enhanced green fluorescent protein (EGFP) sequence can be found in Table S2, and its expression and purification protocol was carried out using the same method as described above.

Conventional CRISPR fluorescence reporting assay

A 20 μL Cas12a fluorescence reporting system was consisted of 50 nM LbCas12a or dCas12a, 100 nM crRNA, 0.5 U/μL RNase inhibitor, 750 nM fluorescence reporter, 2 μL samples (ssDNA, dsDNA, or amplification products), and 1× NEBuffer 2.1. The mixture was transferred to a 384-well plate for reaction at 37 °C, and the fluorescence intensity was read every 3 min (λ_{Ex}: 535 nm, λ_{Em}: 556 nm).

Table S1. Oligonucleotides used in this study

Name	Sequences (5'-3')
Mimic target-F	ATTAGGGATTATGGAAAACAGATGGCAGGTGA TGATTGTGTGGCAAGAAAACAG
Mimic target-R	CTGTTTTCTTGCCACACAATCATCACCTGCCAT CTGTTTTCCATAATCCCTAAT
Trans-F	TAATACGACTCACTATAGGGTAATTTCTACTAA GTGTAGATTTGCCACACAATCATCACCT
Trans-R	AGGTGATGATTGTGTGGCAAATCTACACTTAGT AGAAATTACCCTATAGTGAGTCGTATTA
HIV-1-crRNA	UAAUUUCUACUAAGUGUAGAUUUGCCACACA AUCAUCACCU
RT-RAA-FP	Biotin-TTTTCGGGTTTATTACAGGGACAGCAGAAA
RT-RAA-RP	ATGTTCTAATCCTCATCCTGTCTACTTGCC
RT-RAA-RP-PAM	ATGTTCTAATCCTCATCCTGTTTTCTTGCC
qRT-PCR-FP	ACAGCAGTACAAATGGC
qRT-PCR-RP	TCCCTGTAATAAACCCGAAAAT
qRT-PCR-Probe	FAM-ATTGGGGGGTACAGTGCAGGGGAA-MGB
Fluorescence reporter	HEX-NNNNNNNNNNN-BHQ_1

*PAM sites in the template strand or non-template strand of mimic target sequences were marked in blue.

*Bases in the RT-RAA-RP that were subjected to mismatch design to introduce the PAM site were annotated in purple.

Table S2. Sequences of the proteins used in this study

Name	Sequences (N-C)
DNase-dead Cas12a (dCas12a)	HHHHHHSSGLVPRGSHMASMTGGQQMGRGSEFMLK NVGIDRLDVEKGRKNMSKLEKFTNCYSLSKTLRFKAIP VGKTQENIDNKRLLVEDEKRAEDYKGVKKLLDRYYL SFINDVLHSIKLKNLNNYISLFRKKTRTEKENKELENLE INLRKEIAKAFKGNEGYKSLFKKDIIETILPEFLDDKDEI ALVNSFNGFTTAFTGFFDNRENMFSEEAKSTSIAFRCIN ENLTRYISNMDIFEKVDAIFDKHEVQEIKEKILNSDYDV EDFFEGEFFNFVLTQEGIDVYNAIIGGFVTESGEKIKGL NEYINLYNQKTKQKLPKFKPLYKQVLSDRESLSFYGE GYTSDEEVLEVFRNTLNKNSEIFSSIKKLEKLFKNFDEY SSAGIFVKNGPAISTISKDIFGEWNVIRDKWNAEYDDIH LKKKAVVTEKYEDDRRKSFKKIGSFSLEQLQEYADAD LSVVEKLKEIIIQKVDEIYKVYGSSEKLFDADFVLEKSL KKNDAVVAIMKDLLDSVKSFENYIKAFFGEGKETNRD ESFYGDFVLAYDILLKVDHIYDAIRNYVTQKPYSKDKF

	KLYFQNPQFMGGWDKDKETDYRATILRYGSKYYLAI MDKKYAKCLQKIDKDDVNGNYEKINYKLLPGPNKML PKVFFSKKWMAYYNPSEDIQKIYKNGTFKKGDMFNL NDCHKLIDFFKDSISRYPKWSNAYDFNFSETEKYKDIA GFYREVEEQGYKVSFESASKKEVDKLVEEGKLYMFQI YNKDFSDKSHGTPNLHTMYFKLLFDENNHGQIRLSGG AELFMRRASLKKEELVVHPANSPIANKNPDNPKKTTT LSYDVYKDKRFSEDQYELHIPIAINKCPKNIFKINTEVR VLLKHDDNPYVIGIDRGERNLLYIVVVDGKGNIVEQYS LNEIINNFNGIRIKTDYHSLLDKKEKERFEARQNWTSIE NIKELKAGYISQVVHKICELVEKYDAVIALADLNSGFK NSRVKVEKQVYQKFEKMLIDKLNYMVDKKSNPCATG GALKGYQITNKFESFKSMSTQNGFIFYIPAWLTSKIDPS TGFVNLLKTKYTSIADSKKFISSFDRIMYVPEEDLFEFA LDYKNFSRTDADYIKKWKLYSYGNRIRIFRNPKKNNV FDWEEVCLTSAYKELFNKYGINYQQGDIRALLCEQSD KAFYSSFMALMSLMLQMRNSITGRTDVDFLISPVKNS DGIFYDSRNYEAQENAILPKNADANGAYNIARKVLWA IGQFKKAEDEKLDKVKIAISNKEWLEYAQTSVKH
Enhanced green fluorescent protein (EGFP)	HHHHHHSSGLVPRGSHMASMTGGQQMGRGSMVSKG EELFTGVVPILVELDGDVNGHKFSVSGEGEGDATYGK LTLKFICTTGKLPVPWPTLVTTLTYGVQCFSRYPDHMK QHDFFKSAMPEGYVQERTIFFKDDGNYKTRAEVKFEG DTLVNRIELKGIDFKEDGNILGHKLEYNYNSHNVYIMA DKQKNGIKVNFKIRHNIEDGSVQLADHYQQNTPIGDG PVLLPDNHYLSTQSALSKDPNEKRDHMVLLEFVTAAG ITLGMDELYK

*Protein sequence of dCas12a is annotated in yellow, with the E925A mutation site highlighted in red.

*Protein sequence of EGFP is annotated in green.

Table S3. Cutting power and speed of the laser cutting machine

PMMA layers	Thickness (mm)	Cutting power (%)	Cutting speed (mm/s)
Top layer	0.5	10	20
2nd layer	1.0	15	20
3rd layer	2.0	20	20
Bottom layer	0.5	10	20

*Laser power of the equipment is 100 W.

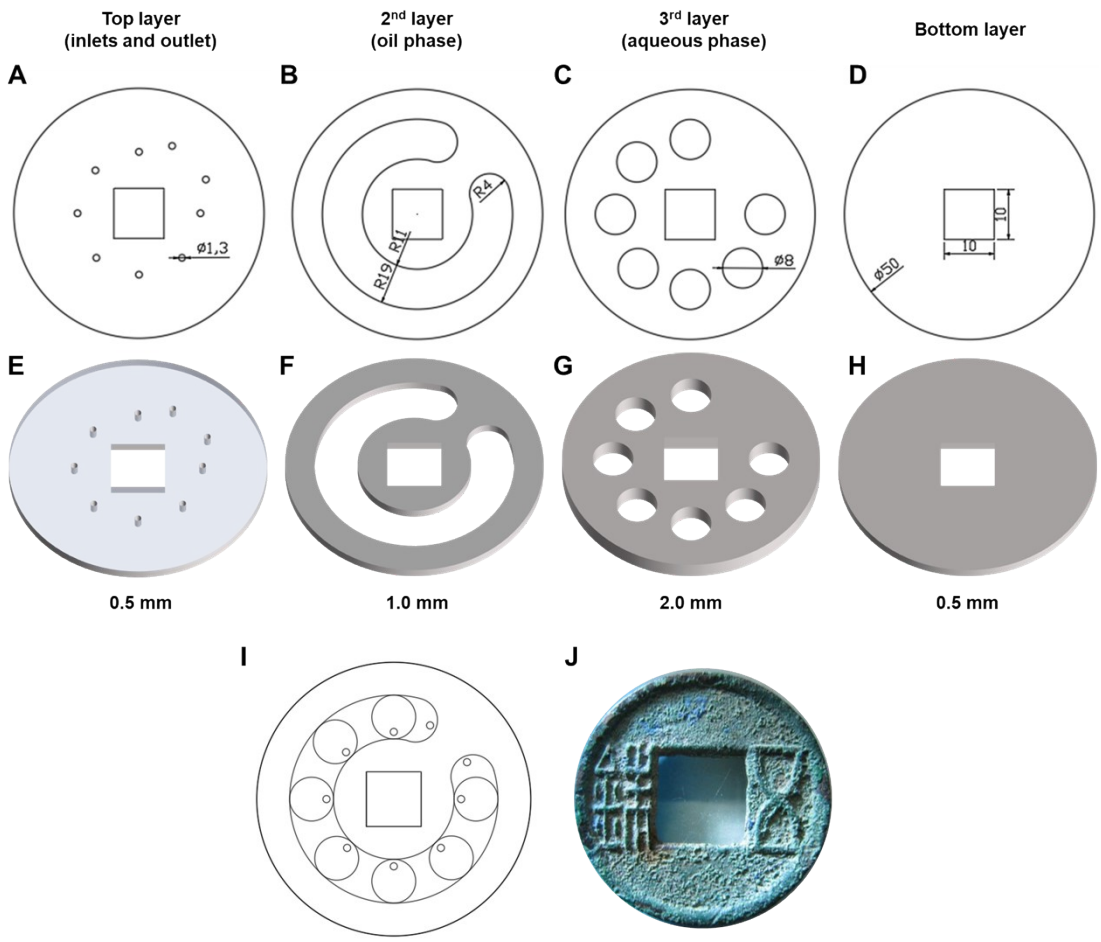

Figure S1. Design concept of the up & down chip structure. (A)-(D) Design diagrams of the top layer, 2nd layer, 3rd layer, and bottom layer in the up and down chip. (E)-(F) model diagrams of each layer in the up and down chip. (I) Design diagram of the up and down chip after assembling. (J) "A circular heaven and a square earth" design concept of the chip, resembling that of ancient Chinese coins.

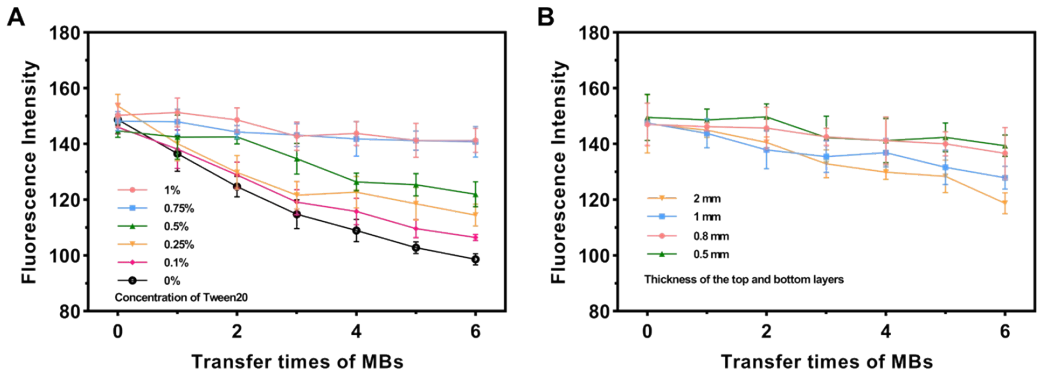

Figure S2. Optimization of the migration efficiency of MBs. (A) The impact of surfactant concentration on the migration efficiency of MBs. The migration efficiency improved with an increase in surfactant concentration. A moderate concentration of 0.75% was selected for subsequent practical use since excessively high concentrations could potentially affect the reaction. (With three technical replicates.) (B) The impact of the thicknesses of the top and bottom layers on the migration efficiency of MBs. A thickness of less than 1 mm for both layers resulted in an improvement in migration efficiency and 0.5 mm was selected for subsequent practical use. (With three technical replicates.)

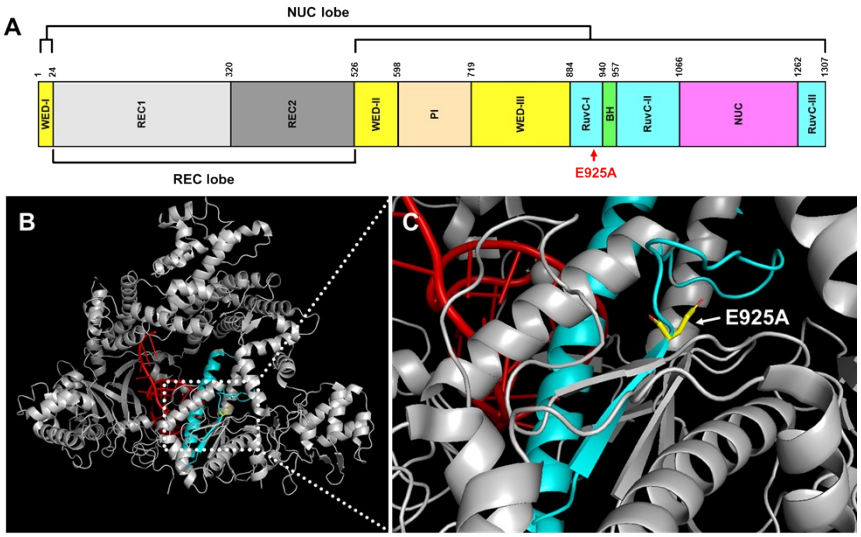

Figure S3. Structural and mutation site analysis of dCas12a. (A) Domain organization of dCas12a. (B), (C) Structural simulation of dCas12a with the E925A mutation site occurred in the RuvC domain of the NUC lobe.

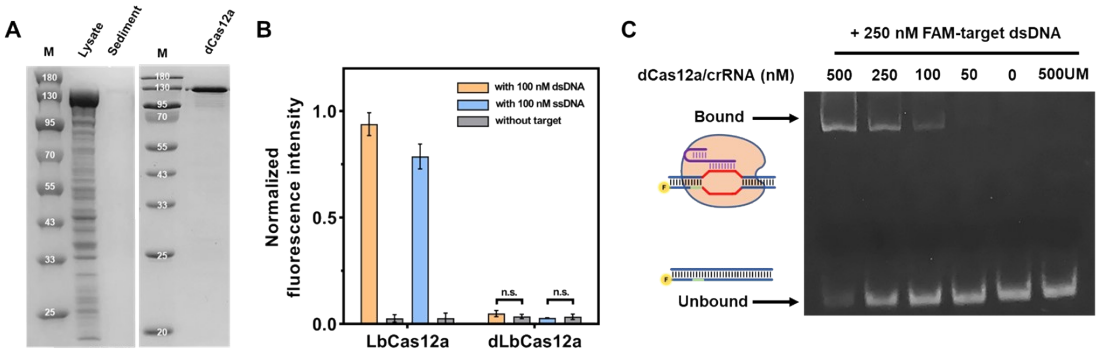

Figure S4. Expression and characterization of dCas12a. (A) SDS-PAGE characterization of dCas12a before and after purification. (B) Conventional CRISPR fluorescence reporting assay for characterizing the *trans*-cleavage activity of dCas12a. The mutated dCas12a no longer possessed the DNase-like activity mediated by crRNA. (With three technical replicates. "n.s.": no significance in "Student's t test".) (C) Native PAGE characterization of the specific binding ability to target DNA of dCas12a. The mutated dCas12a still retained the ability to specifically recognize and bind target DNA mediated by crRNA.

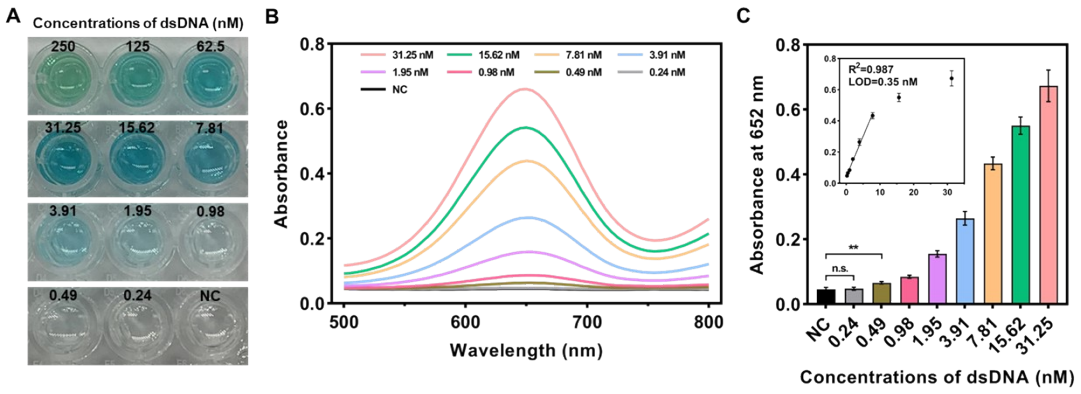

Figure S5. Feasibility characterization of nucleic acid detection using dCas12a-functionalized MBs. (A) Response of color changes vs. different concentrations of target dsDNA by dCas12a-functionalized MBs. The color change directly visible to the naked eye was observed at 0.98 nM target dsDNA. (B) Full-wavelength scans of each reaction group showed a maximum absorption peak at 652 nm. (C) Response of the absorption values at 652 nm vs. different concentrations of target dsDNA by dCas12a-functionalized magnetic beads. A color change that can be directly detected by a plate reader was observed at 0.49 nM target dsDNA. (With three technical replicates. **p < 0.01. “n.s.”: no significance in “Student’s t test”).

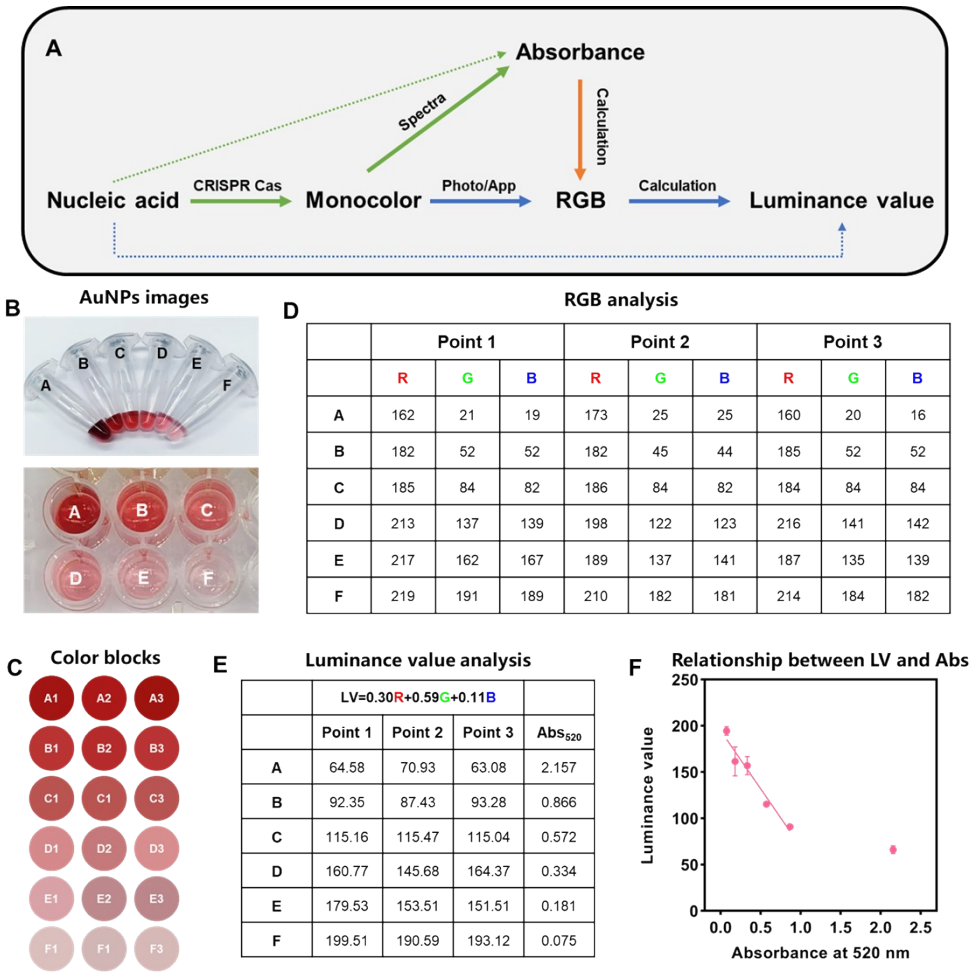

	Point 1			Point 2			Point 3		
	R	G	B	R	G	B	R	G	B
A	162	21	19	173	25	25	160	20	16
B	182	52	52	182	45	44	185	52	52
C	185	84	82	186	84	82	184	84	84
D	213	137	139	198	122	123	216	141	142
E	217	162	167	189	137	141	187	135	139
F	219	191	189	210	182	181	214	184	182

Figure S6. Feasibility characterization of signal output based on image analysis. (A) The basic principle of signal transduction and output. The monocolor signal generated by the CRISPR Cas detection system was converted into the RGB values by the image recognition APP and then converted into luminance values using the corresponding formula. (B) Images of different concentrations of AuNPs solution. (C) Color blocks extracted from the images of different concentrations of AuNPs solution. (D) RGB values extracted from the color blocks using the APP. (E) Calculation of the luminance values of the color blocks using the formula (LV = 0.30R + 0.59G + 0.11B). (F) Correspondence between the luminance values and the absorbance of AuNPs at 520 nm, indicating the feasibility of using luminance analysis based on image recognition as a signal output method. (With three technical replicates.)

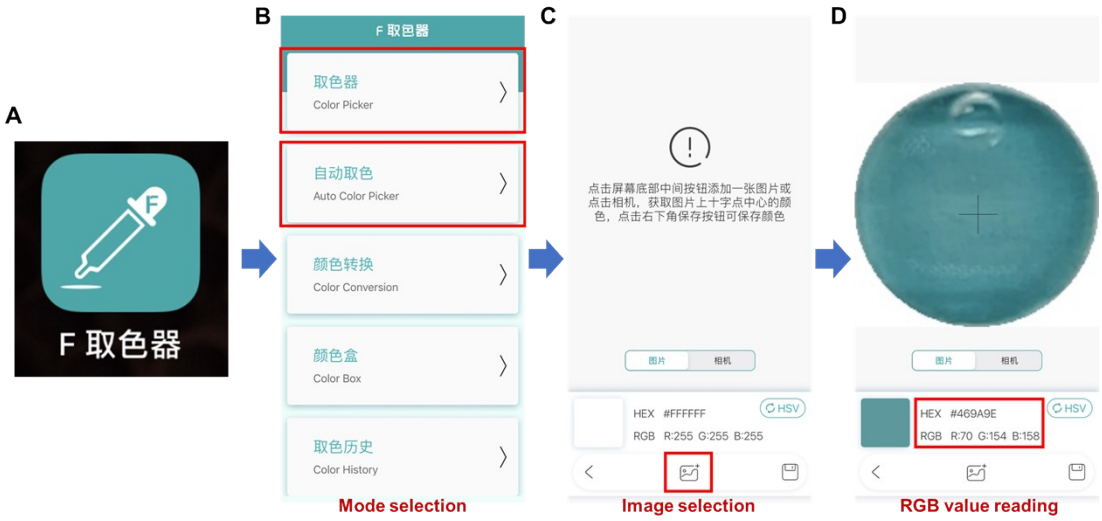

Figure S7. Operation procedures of the image recognition APP. (A) Free image recognition APP. (B) Selection of the color-picking method (manual or automatic). (C) Selection of the image to be recognized. (D) Reading of RGB values in the image color blocks.

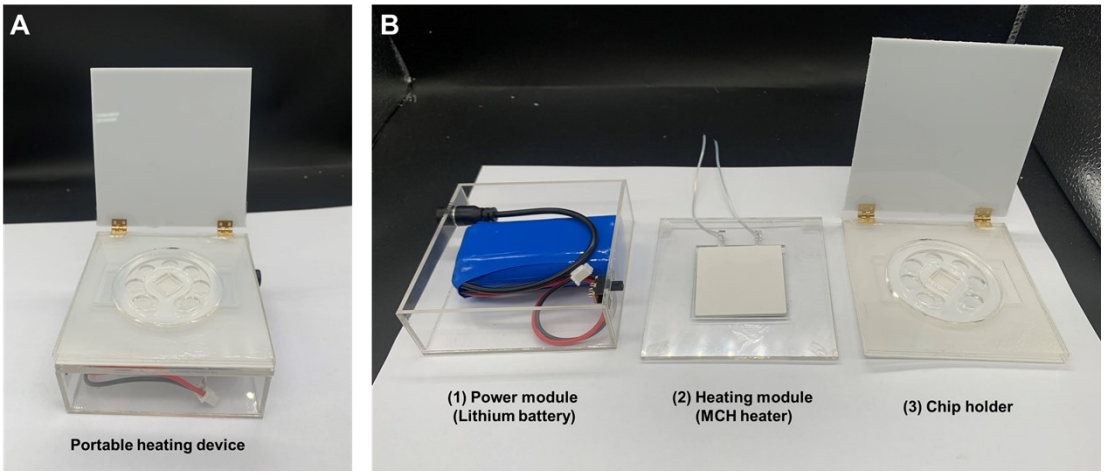

Figure S8. Design of the homemade portable heating box. (A) Image of the homemade portable heating box. (B) Disassembly of the structure of this heating box. It consisted of a power module, a heating module, and a chip holder.

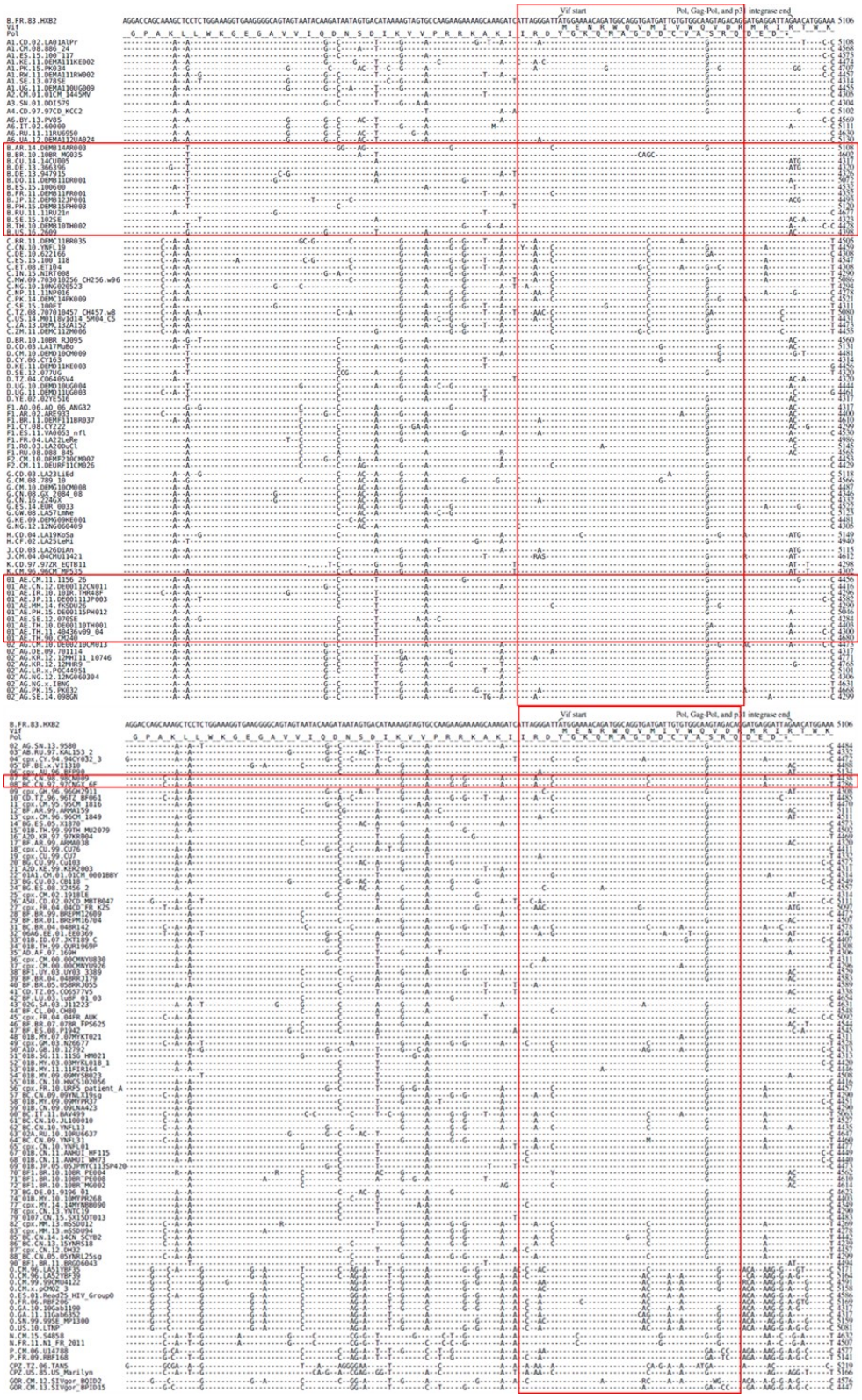

Figure S9. Alignment of HIV-1 genomic sequences from different subtypes (data from the Los Alamos National Laboratory). The relatively conserved gene segment of HIV-1 that we selected was framed by the long rectangle, and the currently prevalent HIV-1 subtypes were framed by the wide rectangle.

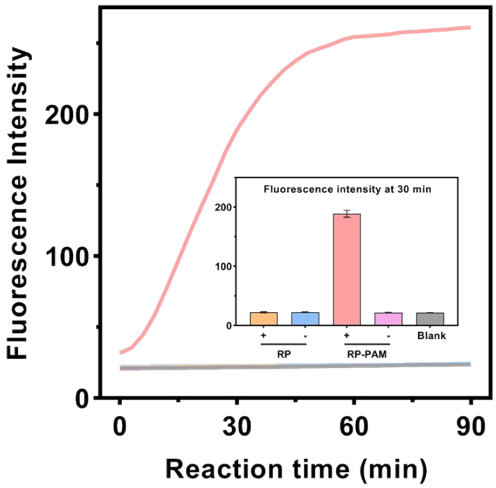

Figure S10. Feasibility characterization of introducing PAM sites during RT-RAA. Different RT-RAA amplification products were tested using the conventional CRISPR fluorescence reporting assay. Only the RP-PAM amplification product produced a significant fluorescent signal in the detection, as it caused some bases in the characteristic fragment to be replaced during the amplification process, forming an artificial PAM site for the recognition by Cas12a. (With three technical replicates.)

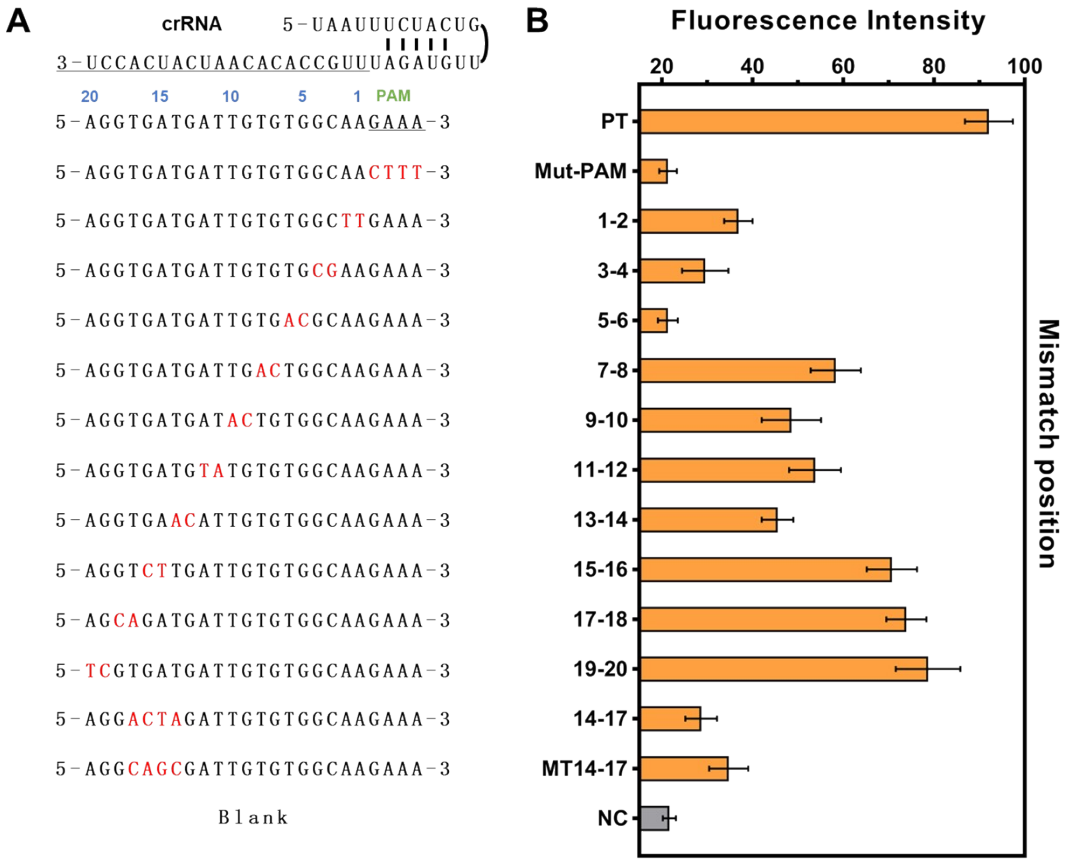

Figure S11. Conservation of the binding and cleavage activities of Cas12a. (A) Mismatches between the crRNA and dsDNA. (B) Fluorescent signals generated by each target dsDNA in the conventional CRISPR fluorescence reporting assay. (With three technical replicates.) Mismatches between the crRNA and dsDNA target affected the binding ability of Cas12a, resulting in a slowed *trans*-cleavage rate, with a greater impact caused by PAM mutations or mismatches in the PAM-adjacent "seed region".

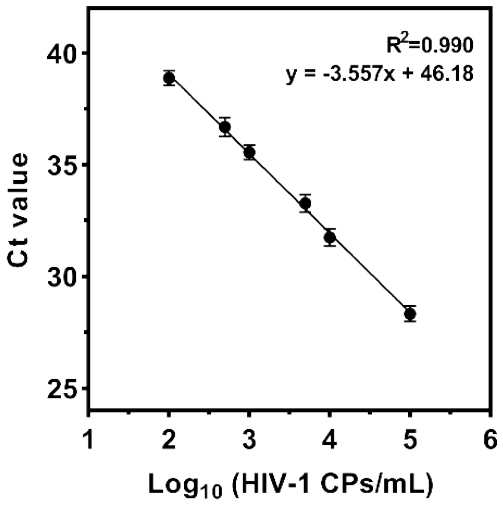

Figure S12. qRT-PCR assays for the comparison with the up & down chip. A qRT-PCR system for HIV-1 using primers and probe according to the National Guideline for Detection of HIV/AIDS (2020) was established to investigate the detection accuracy of the up & down chip. (The standard curve: $Y = -3.557 \times \log_{10}(X) + 46.18$, $R^2 = 0.990$, Y: the Ct values; X: the concentrations of HIV-1 (CPs/mL)).

Table S4. Detection results of spiked samples

No.	Spiked (CPs/mL)	qRT-PCR							up & down chip					
		Ct value				Calculated (CPs/mL)	Recovery (%)	Diagnosis (P/N) [a]	Luminancevalue				ΔLV	Diagnosis (P/N) [b]
		Ct1	Ct2	Ct3	Average				LV1	LV2	LV3	Average		
1	800	36.257	35.809	35.711	35.926	763.590	95.4	P	187.88	185.88	193.70	189.15	16.96	P
2	0	-	-	-	-	-	-	N	203.78	206.78	207.00	205.85	0.26	N
3	900	35.827	35.209	36.204	35.747	857.400	95.3	P	184.70	178.50	187.06	183.42	22.69	P
4	6000	33.061	32.957	32.721	32.913	5368.198	89.5	P	163.22	156.22	165.22	161.55	44.56	P
5	300	37.452	37.166	37.829	37.482	278.757	92.9	P	201.80	195.10	199.50	198.80	7.31	P
6	600	36.598	36.011	36.638	36.416	556.037	92.7	P	196.40	199.50	198.10	198.00	8.11	P
7	0	-	-	-	-	-	-	N	205.22	207.22	208.45	206.96	-0.85	N
8	0	-	-	-	-	-	-	N	203.78	205.22	209.08	206.03	0.09	N
9	400	37.249	37.461	36.925	37.212	332.139	83.0	P	194.48	198.57	196.09	196.38	9.73	P
10	0	-	-	-	-	-	-	N	206.78	204.67	204.96	205.47	0.64	N
11	0	43.891	-	-	-	-	-	N	206.67	208.56	204.00	206.41	-0.30	N
12	0	-	43.347	-	-	-	-	N	205.88	206.00	205.58	205.82	0.29	N
13	0	-	-	-	-	-	-	N	206.40	208.99	206.22	207.20	-1.09	N
14	750	36.225	36.004	35.874	36.034	711.721	94.9	P	192.30	177.70	196.00	188.67	17.45	P
15	1000	35.823	35.490	35.598	35.637	920.481	92.0	P	174.21	176.88	184.10	178.40	27.72	P
16	0	-	-	-	-	-	-	N	206.78	208.78	204.11	206.56	-0.44	N
17	5000	33.408	32.979	32.909	33.099	4760.263	95.2	P	161.81	167.52	163.22	164.18	41.93	P
18	0	-	-	-	-	-	-	N	208.30	206.18	203.99	206.16	-0.04	N
19	500	36.904	36.887	36.480	36.757	445.803	89.2	P	196.50	201.67	197.08	198.42	7.70	P
20	0	-	-	-	-	-	-	N	207.78	205.60	209.00	207.46	-1.35	N
21	3000	33.987	33.512	34.187	33.895	2842.232	94.7	P	161.11	176.30	172.92	170.11	36.00	P
22	0	-	-	-	-	-	-	N	208.00	205.82	206.22	206.68	-0.57	N
23	0	-	43.233	-	-	-	-	N	208.31	208.78	206.78	207.96	-1.84	N
24	6000	32.857	32.492	33.251	32.867	5531.647	92.2	P	162.73	166.72	162.02	163.82	42.29	P
25	7000	32.342	32.876	32.703	32.640	6404.495	91.5	P	158.32	162.73	165.32	162.12	43.99	P
26	0	-	-	-	-	-	-	N	205.22	206.58	204.00	205.27	0.85	N
27	7500	32.270	32.405	32.751	32.475	7126.434	95.0	P	162.28	158.41	159.61	160.10	46.01	P
28	0	-	-	-	-	-	-	N	206.07	207.38	206.78	206.74	-0.63	N
29	1000	35.302	35.997	35.714	35.671	900.443	90.0	P	178.88	179.48	172.70	177.02	29.09	P
30	0	-	-	-	-	-	-	N	204.45	207.00	208.78	206.74	-0.63	N
31	0	42.962	-	-	-	-	-	N	204.00	205.11	204.89	204.67	1.45	N
32[d]	250	38.089	37.521	37.749	37.786	228.960	91.6	P	202.99	201.74	202.81	202.51	3.60	N
33	5000	33.183	33.225	32.874	33.094	4774.665	95.5	P	162.04	175.22	156.93	164.73	41.38	P
34	0	-	-	-	-	-	-	N	202.00	206.78	204.74	204.51	1.61	N
35	100000	28.578	28.741	28.384	28.568	89424.644	89.4	P	148.37	143.78	153.75	148.63	57.48	P
36	0	-	-	-	-	-	-	N	205.60	206.78	204.67	205.68	0.43	N
37	10000	31.967	31.872	32.370	32.070	9266.584	92.7	P	156.05	155.93	156.44	156.14	49.97	P
38	0	-	43.721	-	-	-	-	N	205.78	204.67	204.33	204.93	1.19	N
39	0	-	-	-	-	-	-	N	206.78	207.07	204.67	206.17	-0.06	N
40	8000	32.514	32.281	32.647	32.481	7101.873	88.8	P	159.58	161.85	160.40	160.61	45.50	P
41	0	-	-	-	-	-	-	N	207.22	206.40	207.93	207.18	-1.07	N
42	2500	34.025	34.483	34.457	34.322	2156.760	86.3	P	178.72	176.42	173.82	176.32	29.79	P
43	700	36.141	35.802	36.270	36.071	695.027	99.3	P	184.48	188.20	176.90	183.19	22.92	P
44	0	-	-	-	-	-	-	N	206.07	206.40	205.00	205.82	0.29	N
45	600	36.215	36.552	36.539	36.435	549.003	91.5	P	189.18	190.66	192.08	190.64	15.47	P
46	2000	34.586	34.418	34.820	34.608	1791.857	89.6	P	176.80	175.02	178.72	176.85	29.27	P
47	0	-	-	-	-	-	-	N	203.89	201.78	204.18	203.28	2.83	N
48	300	37.417	37.656	37.483	37.519	272.277	90.8	P	197.43	199.46	201.28	199.39	6.72	P
49	0	42.065	-	-	-	-	-	N	204.78	204.89	203.78	204.48	1.63	N
50	0	-	-	-	-	-	-	N	203.99	208.31	207.60	206.63	-0.52	N
51	1000000	25.085	25.124	25.539	25.249	766230.577	76.6[c]	P	147.32	146.05	146.87	146.75	59.37	P
52	0	-	-	-	-	-	-	N	205.71	207.00	208.78	207.16	-1.05	N
53	0	-	43.775	-	-	-	-	N	207.82	204.78	206.89	206.50	-0.38	N
54	9000	32.976	31.801	32.064	32.280	8085.256	89.8	P	159.13	159.81	156.99	158.64	47.47	P
55	10000	32.551	31.780	31.891	32.074	9240.627	92.4	P	158.71	161.28	158.70	159.56	46.55	P
56	0	-	-	42.684	-	-	-	N	208.67	204.78	206.97	206.81	-0.69	N

[a] Judged as “Negative” when the Ct value was larger than 42 or undetected.

[b] Average ΔLV (6.08) of the negative control signal plus three times the standard deviation was set as the cut-off line for diagnosis. Judged as “Positive” when the ΔLV was larger than this cut-off line.

[c] Reason for the low recovery rate of sample 51 was that its concentration was outside the dynamic detection range of qRT-PCR, thereby preventing its effective quantification.

[d] Regarding sample 32, two detection methods exhibited different results, and the reasons for this discrepancy were discussed in the main text.

Table S5. Cost analysis of different methods for HIV-1 diagnosis

	Method	Manufacturer	Reagents cost ($/sample)	Concumables cost ($/sample)	Total cost without instruments ($/sample)	Instruments/ device cost ($)
1	qRT-PCR	Thermo Fisher/ TsingKe	Pretreatment kit (2.75) + qRT-PCR kit (5.50) + primers and probe (2.06) = 10.31	1.11	11.42	qRT-PCR thermocycler (> 30000.00)
2	Up & down chip	Our assay	Pretreatment kit (2.75) + RT-RAA kit (2.75) + dCas12a-MBs (1.10) + others (2.50) = 9.10	1.37	10.47	Heating box (1.10) + smartphone (275.00) = 276.10